HIRDLS

TR-LOC-711
Rev. A

HIGH RESOLUTION DYNAMICS LIMB SOUNDER

Originators: Jonathan K. Chow Date: 2000 October 29

Subject/Title: **An Analysis of the Impact of the Encoder Non-linearity on the Relative Knowledge of Elevation**

Description/Summary/Contents:

This document contains an estimate of the impact of the elevation encoder small-scale non-linearity on Relative Knowledge Error in elevation. Experimental data obtained using the elevation encoders on the Proto-Flight Model (PFM) Scanner was used to provide this assessment. An estimate of the calibration curve needed to characterize the small-scale non-linearity was found. The knowledge error residue from the calibration, otherwise known as the random error, was found to be significant in comparison to the calibration curve. Thus, calibration will not eliminate the dependence of the Relative and Absolute Knowledge Errors on the encoder non-linearity and further filtering of the science data will be necessary to reduce the impact of this source of error.

Keywords: LOS knowledge, Scanner, Proto-Flight Model, Elevation, Encoder Nonlinearity

Purpose of this Document: (20 char max.) Summarize the errors in elevation knowledge performance due to the limited accuracy of elevation encoders

Reviewed/Approved by: Date (yy-mm-dd):			

Palo Alto Advanced Technology Center
CAGE Code 65113
Lockheed Martin Missiles & Space
3251 Hanover Street
Palo Alto, CA 94304-1191
United States of America

EOS

Contents

List of Figures

List of Tables

Executive Summary

This document contains an estimate of the impact of the elevation encoder small-scale non-linearity on Relative Knowledge Error in elevation. Experimental data obtained using the elevation encoders on the Proto-Flight Model (PFM) Scanner was used to provide this assessment. An estimate of the calibration curve needed to characterize the small-scale non-linearity was found and defined to be the Systematic Error. The knowledge error residue from the calibration, otherwise known as the Random Error, was found to be significant in comparison to the calibration curve. Thus, calibration will not eliminate the dependence of the Relative and Absolute Knowledge Errors on the encoder non-linearity and further filtering of the science data will be necessary to reduce the impact of this source of error.

The results presented in this report also show that the systematic error in the Relative Knowledge due to the encoder non-linearity has not significantly improved over the encoder performance observed on the Engineering Model. This phenomenon is also shown to have a frequency that is approximately equal to the cutoff frequency of the Pointing Low-Pass Filter (PLPF) and will impact both the elevation angle pointing and jitter spectra. An estimate of the fringe spacing was also extracted from the data.

Preamble

This report provides an estimate of the elevation encoder nonlinearity and an analysis of the potential impact of calibrating the elevation encoders to mitigate its effects on the random elevation knowledge error. It does not extract the true encoder non-linearity but assumes that the effects exhibited by the two encoders are not correlated in time and can be investigated using the difference between the encoder signals. This report presents the results and conclusions from the analysis of actual measured data.

Description of Data

The data was taken by Drs. Jonathan Chow and Marion Barker during Engineering Confidence tests conducted on the PFM Scanner during the month of September, 2000 at Lockheed Martin ATC:

- The Global Scan Profile described in SP-HIR-198, Table 1 was used to generate the commanded azimuth and elevation angles and rates. The Command Profiles for Elevation and Azimuth Shaft are plotted in Figure 1.
- Read-Head #1 of the Secondary Encoder Electronics Assembly (EEA) was used to control the elevation axis.
- The azimuth controller was OFF except when the azimuth angle was stepped.
- A ‘quiet’ noise test environment was used for this test, i.e.; no external vibration was introduced.

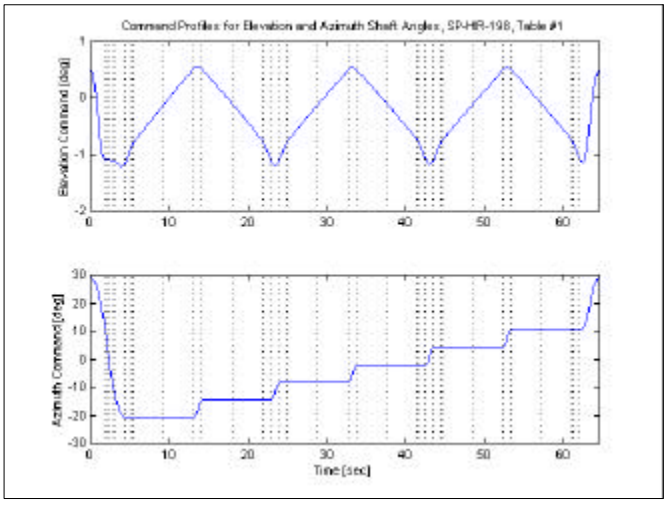

Figure 1: Command Profiles in elevation and azimuth shaft angles, Table 1, SP-HIR-198.

Procedure

1. The read-heads located at the top of each of the yoke arms were chosen for this analysis. These read-heads are defined as Primary EEA Read-Head #1, $q_{1\ primary\_EEA}$ and Secondary EEA Read-Head #2, $q_{1\ secondary\_EEA}$.
2. Relative scale factors and offsets in the read-head outputs were first eliminated with a linear Least Squares Fit using the commanded elevation angle time history as the basis for the fit.
3. The elevation data was reduced to include only the periods when slow elevation scanning was active.
4. The Relative Knowledge Error, $(q_{1\ primary\_EEA} - q_{1\ secondary\_EEA})$, was calculated. A mean offset observed for each scan segment (related to yoke-deformation as a function of azimuth position) was eliminated with the assumption that the encoder non-linearity was not dependent on azimuth position.
5. The resulting corrected Relative Knowledge Error was filtered in the forward and backward directions, using a Chebyshev Type II filter (described below) in order to remove signals whose frequencies were above 120 Hz without phase distortion.
6. The filtered Relative Knowledge Error was then fitted using least-square polynomial methods to the commanded elevation shaft angle. The data was fitted in increments that were approximately 8 arcseconds long using 16^{th}-order polynomials. The resulting curve-fit was the Systematic Error due to the encoder non-linearity and decentred encoder disks. The curve-fit residue was the Random Error.
7. The effects of the decentred disks were removed by detrending the Systematic Error using a high-order polynomial least-squares fit of the commanded elevation shaft angle. The data set was truncated beforehand to reduce 'edge effects' associated with transients from commanded changes in the elevation shaft angular rates. The detrended Systematic Error is the estimated calibration curve necessary to reduce the effects of the encoder non-linearity.
8. The pointing spectrum of the Random Error was found with the Pointing Low Pass Filter (PLPF). [1]
9. The power spectrum of the Systematic Error was calculated with a method that left the RMS values in the time and frequency domains equal.[2] The encoder non-linearity is related to the fringe spacing in the encoder. An estimate of the fringe spacing was generated using the location of the frequencies associated with the resonance peaks and the elevation scan rate.

Filters:
In this analysis, a Chebyshev Type II filter was used to isolate the error associated with the encoder non-linearity instead of the PLPF. The PLPF will significantly distort the phase and magnitude of signals with frequencies between 20-80 Hz. The apparent frequency of the phenomena associated with the encoder non-linearity is approximately 37 Hz (see Figure 8). The effect of the PLPF on the Relative Knowledge Error can be seen in Figure 2. The top panel plots the Relative Knowledge Error as a function of the commanded elevation angle, prior to filtering with the PLPF. The bottom panel plots the PLPF-filtered error.

A Chebyshev Type II filter with a corner frequency around 120 Hz was applied to the data prior to the determination of Systematic Error. Figure 3 shows the frequency response of the Chebyshev filter. The data was filtered in the forward and backward directions for zero-phase distortion. Figure 4 shows the results of this process. The specifications of both the PLPF and Chebyshev filters are given in Table 1.

	Pointing Low-Pass Filter (PLPF)	**Chebyshev Type II Filter**
Order	8	9
Corner Frequency	36 Hz.	116 Hz.
Stopband Ripple Magnitude	-	40 dB

Table 1: Filter specifications.

[1] Formally defined in the Instrument Technical Specification (ITS) as an 8-pole Butterworth-type low-pass filter with a corner frequency of 36 Hz.
[2] Various methods had been investigated and it was found that rectangular windowing was the best option. The power spectrum was normalized to represent a double-sided PSD.

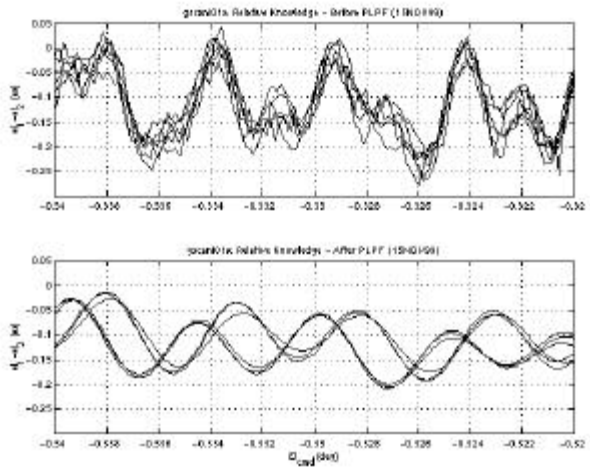

Figure 2: The effect of the PLPF on the Relative Knowledge Error.

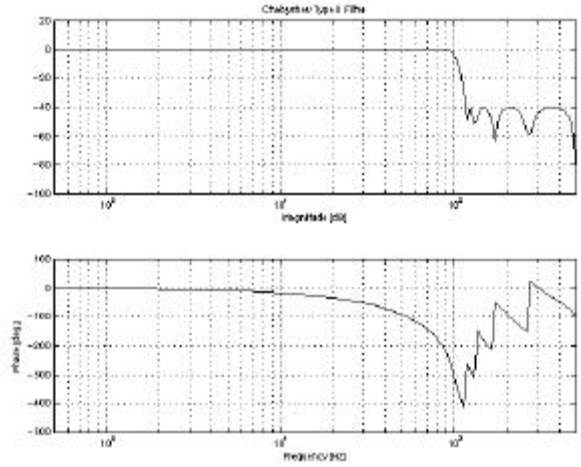

Figure 3: The frequency response of the Chebyshev Type II Filter.

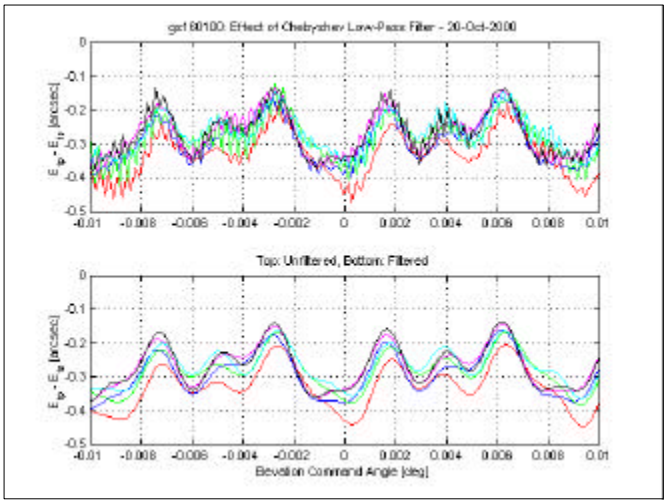

Figure 4: The effect of the Chebyshev Type II filter on the Relative Knowledge Error.

Discussion of Results

The relative difference between two read-head outputs was observed to be dependent on azimuth position, encoder disk decentration, and encoder non-linearity. Figure 5 shows a plot of the relative difference as a function of time during a global scan. The time ticks correspond to scan table entries (please see Figure 1). The relative difference is a function of azimuth position because the elevation read-heads are located on the yoke arms, which will deform statically as the scanner is moved in azimuth. This phenomenon will be explored in greater detail in TC-LOC-712. The impact of the yoke deflection on the relative knowledge is a mean offset that is constant over the elevation range of interest, and can be removed for the purposes of this analysis with the assumption that it has a negligible impact on the encoder non-linearity. The corrected relative error is plotted as a function of the commanded elevation shaft angle in Figure 6. The relative knowledge error is then passed through the Chebyshev Type II filter using a zero-phase-distortion filtering algorithm, as described above in Step 5. The filtered result is plotted against the commanded elevation shaft angle in Figure 7. Figure 8 presents the spectra of the difference between the two read-head measurements. Four distinct sets of peaks can be found in the power spectra shown in Figure 8. One set, centred around 60 Hz is caused by the power supply. The first two sets, i.e., the peaks found between 15-20 and 37-40 Hz, are of interest because they are below or around the cut-off frequency of the Pointing Low-Pass Filter (PLPF) and the bandwidth of the elevation axis controller[3]. The remaining set, around 70-80 Hz, will strongly impact the elevation angle jitter spectrum.

The curve-fit of the relative knowledge error was executed in 8-arcsecond increments with 16^{th}-order polynomials to capture the small-scale nonlinearity and the effects of the decentred encoder disks. This curve-fit is presented in Figure 9. Note that the elevation range used for this portion of the analysis was truncated to eliminate "edge effects," i.e.; distortions in the encoder signal caused by significant changes in the elevation angular rate. Figure 10 presents a close-up of the incremental curve-fit, with the actual data for comparison.

The curve-fit was then detrended with a high-order polynomial to eliminate the effect of encoder disk decentration. This decentration curve is plotted in Figure 11. The resulting detrended curve-fit is the estimated calibration function for the encoder small-scale non-linearity. It is plotted in Figure 12. This calibration curve represents the Systematic Knowledge Error associated with the encoder non-linearity. The root mean square error is 0.065 arcseconds. The band-limited residue from the curve-fitting process is the Random Knowledge Error[4]. It is plotted in Figure 13. The root mean square error is 0.021 arcseconds. This is a significant error in relation to the science requirements, and suggests that *calibration will not reduce the random knowledge error in elevation associated with the encoder non-linearity to the level required without additional filtering*.

The Systematic Error and its pointing spectrum are plotted as a function of frequency in Figure 14 and Figure 15, respectively. The center frequency of each of the peaks found in the plot was determined for each scan and the associated angle was calculated. The results are presented Table 2. The values for Resonance Peak #2 provide an estimate of the spacing between the fringes in the encoders. The other peaks have values that are approximately half and double this value. Comparing these results to those found for the EM encoders[5], the fringes are spaced slightly closer together by about an arcsecond.

Resonance	Scan 1	Scan 2	Scan 3	Scan 4	Scan 5	Scan 6	Average
#1	32.55 as	33.41 as	33.41 as	34.31 as	34.31 as	33.41 as	33.6 ± 0.7 as
#2	16.07 as	16.49 as	16.93 as	16.93 as	16.93 as	16.71 as	16.7 ± 0.3 as
#3	8.04 as	8.04 as	8.46 as	8.52 as	8.35 as	8.35 as	8.3 ± 0.2 as

Table 2: Results from an analysis of the power spectra of the Systematic Error: The fringe spacing corresponding to the resonance peaks.

[3] The bandwidth of the elevation axis controller is approximately 30 Hz.
[4] Stochastic error that is band-limited by passage through the PLPF.
[5] See TC-LOC-444: "Analysis of the Performance of the Engineering Model Scanner."

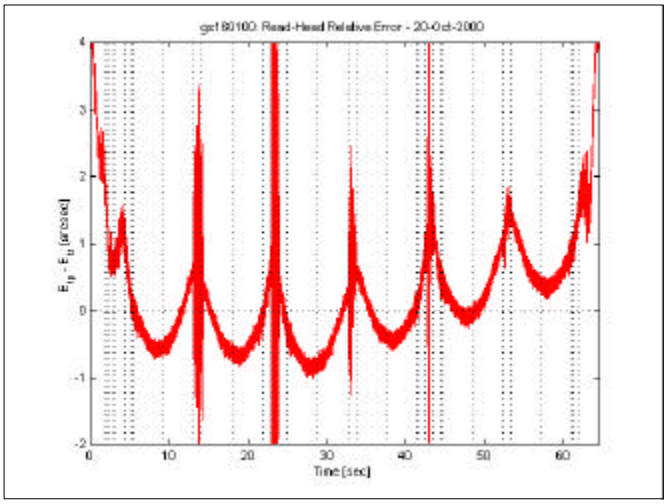

Figure 5: The Relative Knowledge Error, ($q_{1\ primary\_EEA} - q_{1\ secondary\_EEA}$), plotted against time during a Global Scan.

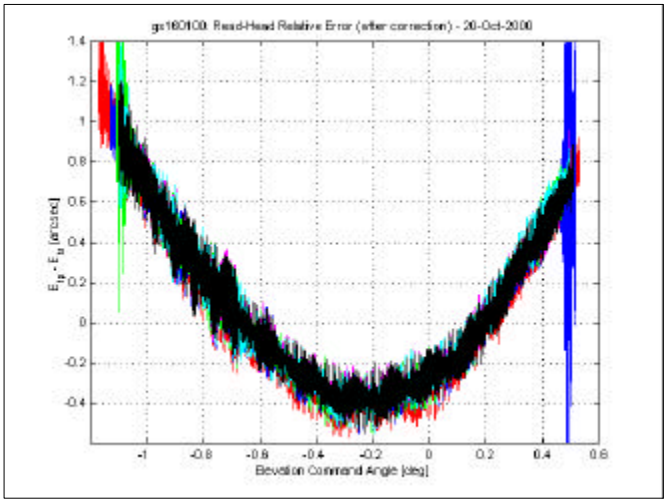

Figure 6: The Relative Knowledge Error plotted against commanded elevation shaft angle.

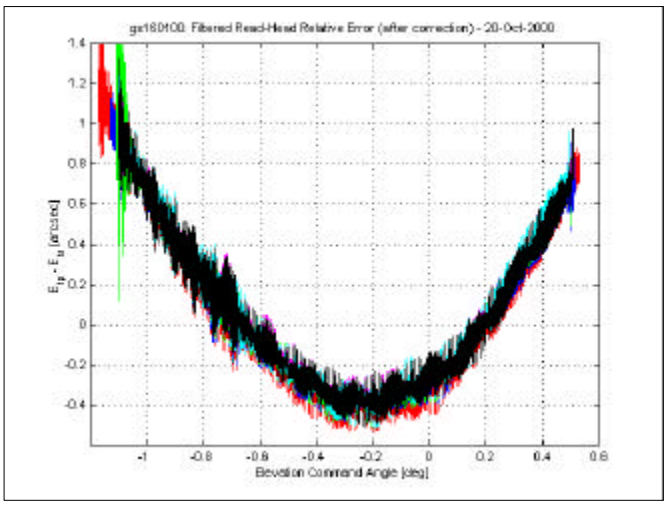

Figure 7: The filtered Relative Knowledge Error plotted against the commanded elevation shaft angle.

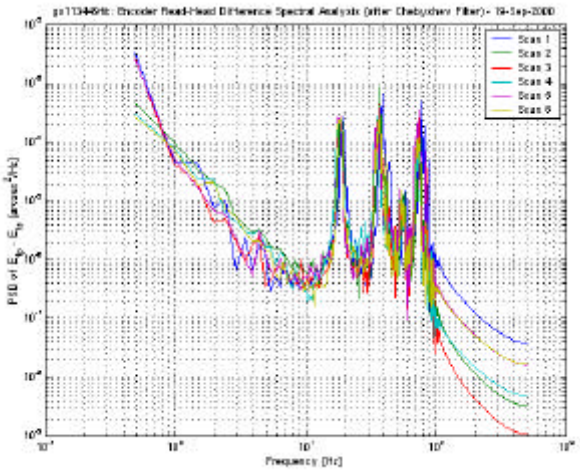

Figure 8: The power spectrum of the Relative Knowledge Error, with Chebyshev-filtering.

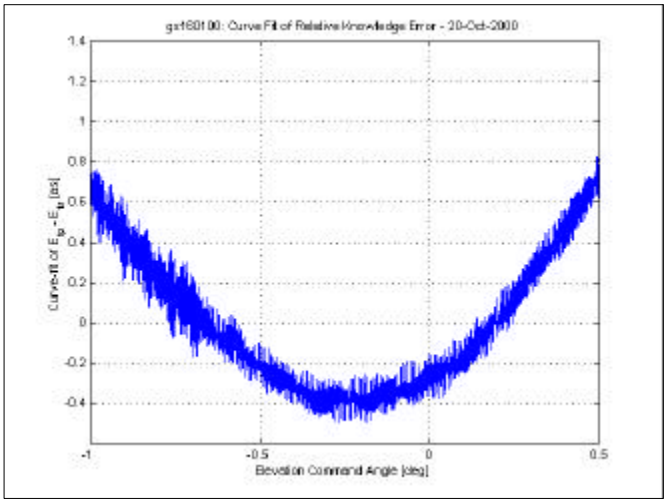

Figure 9: The Fitted Relative Knowledge Error, plotted against the commanded elevation shaft angle.

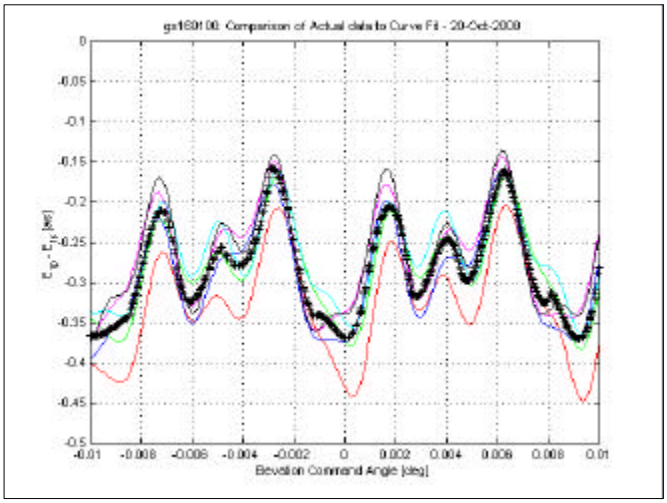

Figure 10: Close-up of the Fitted Relative Knowledge Error, compared against the actual data.

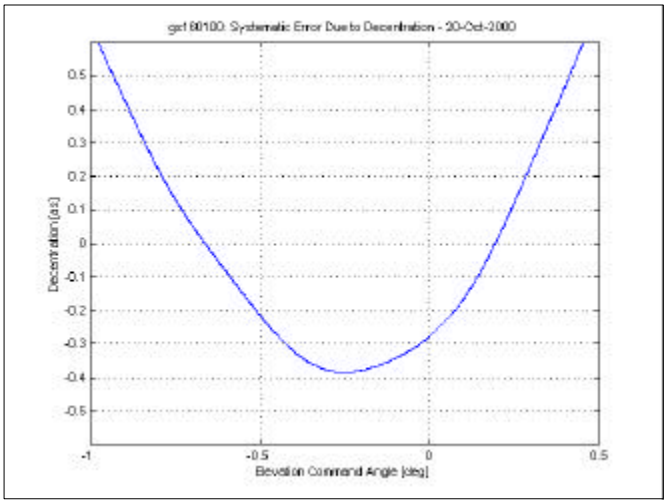

Figure 11: The error due to Encoder Disk Decentration, plotted against commanded elevation shaft angle.

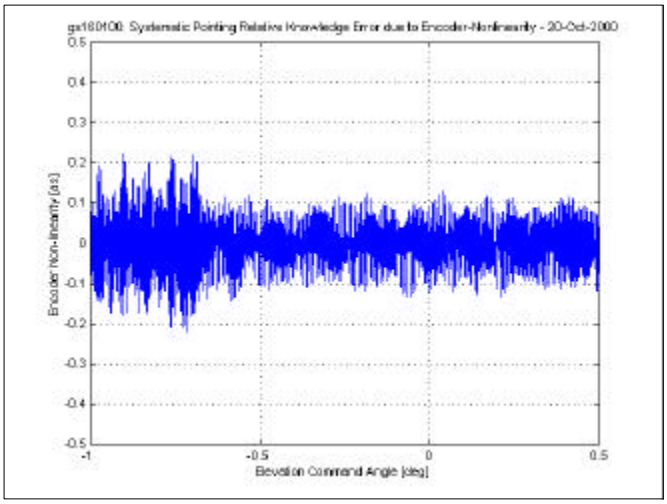

Figure 12: The Estimated Calibration Curve for Encoder Small-Scale Non-linearity, as a function of the commanded elevation shaft angle.

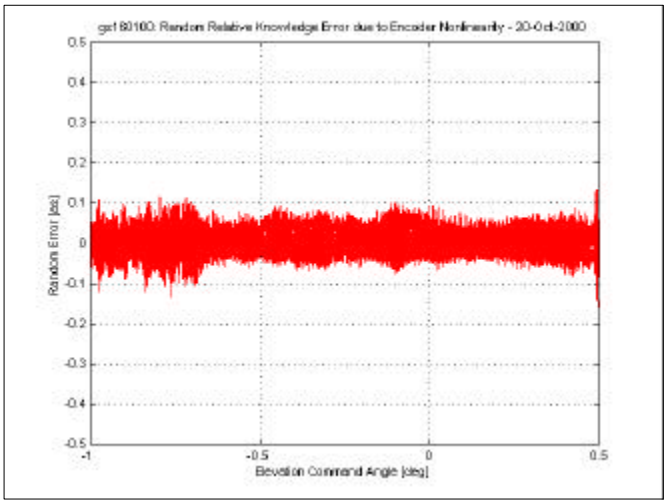

Figure 13: The Random Pointing Relative Knowledge Error associated with the Small-Scale Non-linearity.

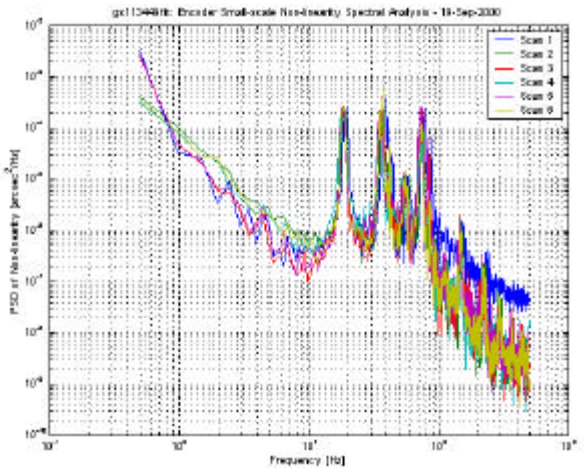

Figure 14: The Power Spectrum of the Systematic Component of the Relative Knowledge, for each scan.

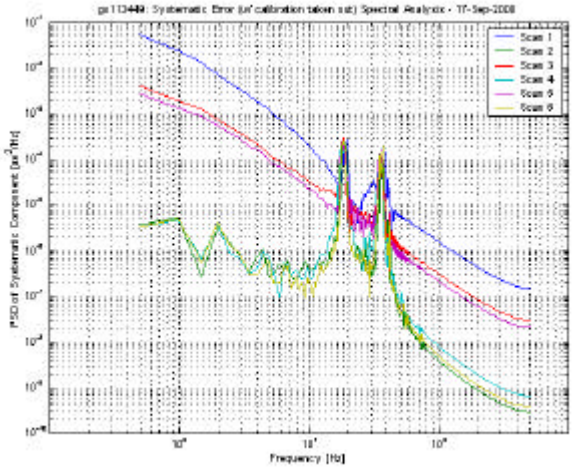

Figure 15: The power spectrum of the Systematic Pointing Relative Knowledge Error, for each scan.

Conclusions

Estimates of the systematic and random errors due to the encoder small-scale non-linearity were determined from the Relative Knowledge Error using data recorded during engineering confidence tests of the PFM Scanner. An estimate of the calibration curve needed to characterize the small-scale non-linearity was found and defined to be the Systematic Error. However, it was shown that the residue from the calibration, otherwise known as the Random Error, was still significant in comparison to the Total Error associated with the phenomenon. Calibration will not eliminate the dependence of the Relative and Absolute Knowledge Errors on the encoder non-linearity. Further processing of the science data will be required to reduce the impact of this Encoder error.

An estimate of the fringe spacing was also extracted from the data.

Appendix A: Test Case

- A simulation of the encoder non-linearity was performed to analyze the effect of a encoder small-scale non-linearity on the control system performance. It investigated whether the Systematic component of the difference between the readings of the two scanner elevation encoders (i.e., the Relative Knowledge Error) can be recovered from the closed-loop data.
- The simulation used an elevation axis open loop transfer function based on measured data and a discrete controller. Figure A. 1 shows the block diagram of the simulation model.
- The encoder non-linearity was introduced to the measurements using the following formula:

$$el_{hi}\,(el_{cmd}) = el_{cmd} + A_{i1}\,Sin(w_{i1}\,el_{cmd} + f_{i1}) + A_{i2}\,Sin(w_{i2}\,el_{cmd} + f_{i2}) + A_{i3}\,Sin(w_{i3}\,el_{cmd} + f_{i3})$$

where: el_{hi} is the output from i^{th} encoder ,
el_{cmd} is the commanded elevation angle,
w_{ij} are based on multiples of the fringe spacing,
A_{i1} , f_{i1} , etc. are arbitrary values.

The results are plotted in Figures A. 2 & A. 3. The true and estimated signals show good correlation in magnitude, but there is a lag due to the presence of the controller. However, it can be concluded that retrieval of the Systematic error of the encoder difference is possible to within 10 to 20% of the actual difference.

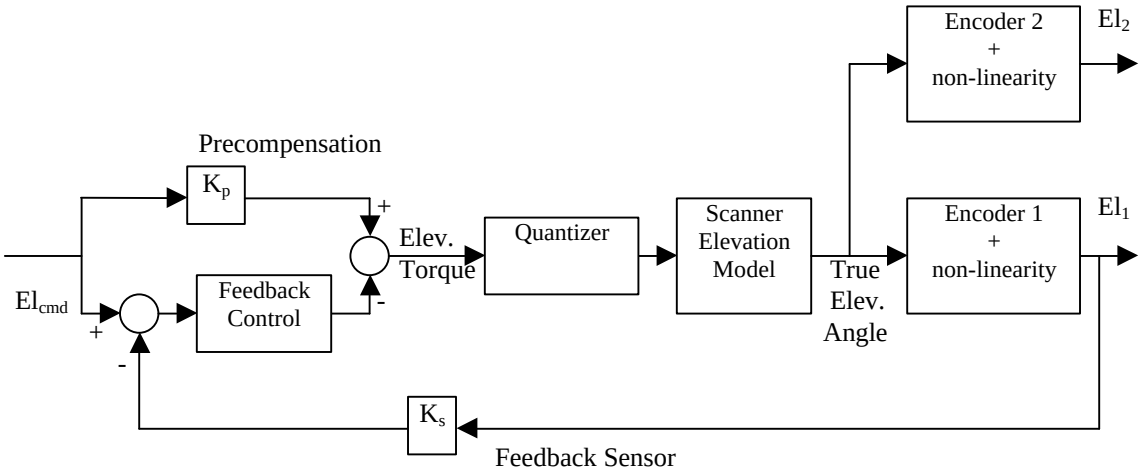

Figure A. 1: Simulation Block Diagram.

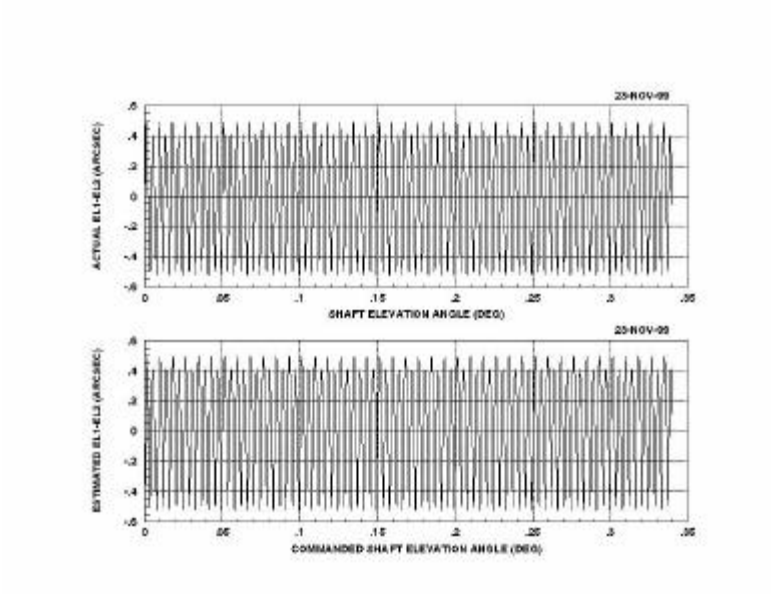

Figure A. 2: Systematic Error plotted as a function of Commanded Elevation Angle. The top panel shows the Actual Error vs. True Shaft Angle. The lower panel shows the Estimated Error vs. Commanded Shaft Angle.

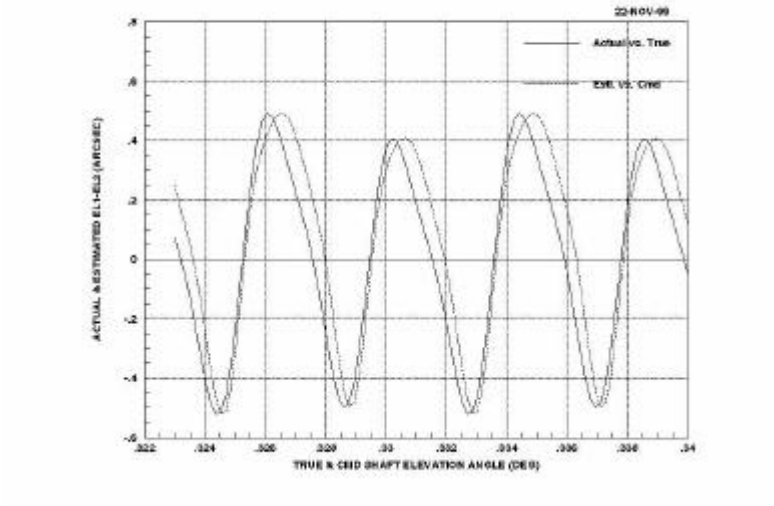

Figure A. 3: Close-up comparison plot showing the phase and magnitude differences between the Actual Error (plotted against True Shaft Angle) and Estimated Error (plotted against Commanded Shaft Angle).